JACS
JOURNAL OF THE AMERICAN CHEMICAL SOCIETY
Article
pubs.acs.org/JACS

TEMPO: A Mobile Catalyst for Rechargeable Li-O_2 Batteries

Benjamin J. Bergner,[†] Adrian Schürmann,[†] Klaus Peppler,[†] Arnd Garsuch,[‡] and Jürgen Janek*[,†]

[†]Institute of Physical Chemistry, Justus-Liebig-Universität Gießen, Heinrich-Buff-Ring 58, 35392 Gießen, Germany
[‡]BASF SE, Carl-Bosch-Straße 38, 67056 Ludwigshafen am Rhein, Germany

Supporting Information

ABSTRACT: Nonaqueous Li-O_2 batteries are an intensively studied future energy storage technology because of their high theoretical energy density. However, a number of barriers prevent a practical application, and one of the major challenges is the reduction of the high charge overpotential: Whereas lithium peroxide (Li_2O_2) is formed during discharge at around 2.7 V (vs Li^+/Li), its electrochemical decomposition during the charge process requires potentials up to 4.5 V. This high potential gap leads to a low round-trip efficiency of the cell, and more importantly, the high charge potential causes electrochemical decomposition of other cell constituents. Dissolved oxidation catalysts can act as mobile redox mediators (RM), which enable the oxidation of Li_2O_2 particles even without a direct electric contact to the positive electrode. Herein we show that the addition of 10 mM TEMPO (2,2,6,6-tetramethylpiperidinyloxyl), homogeneously dissolved in the electrolyte, provides a distinct reduction of the charging potentials by 500 mV. Moreover, TEMPO enables a significant enhancement of the cycling stability leading to a doubling of the cycle life. The efficiency of the TEMPO mediated catalysis was further investigated by a parallel monitoring of the cell pressure, which excludes a considerable contribution of a parasitic shuttle (i.e., internal ionic short circuit) to the anode during cycling. We prove the suitability of TEMPO by a systematic study of the relevant physical and chemical properties, i.e., its (electro)chemical stability, redox potential, diffusion coefficient and the influence on the oxygen solubility. Furthermore, the charging mechanisms of Li-O_2 cells with and without TEMPO were compared by combining different electrochemical and analytical techniques.

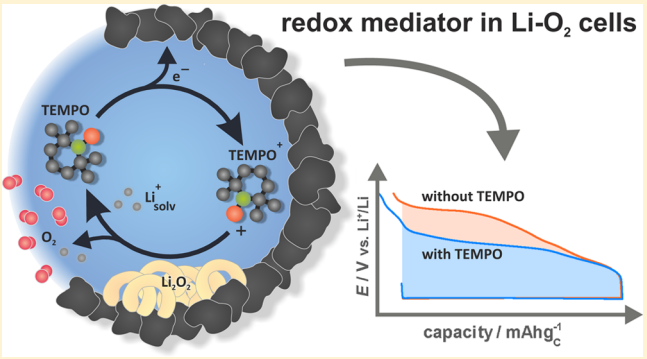

1. INTRODUCTION

In the light of growing research on mobile energy storage systems, aprotic lithium-oxygen (Li-O_2) batteries have recently attracted significant interest.[1−4] Since the active material of the positive electrode, oxygen, can be sourced from the atmosphere, (practical) energy densities up to 900 Wh kg^{-1} have been considered as possible.[5] However, the technical application of Li-O_2 batteries requires the surmounting of several electrochemical, chemical and technical challenges. Major drawbacks are the low round-trip efficiency, the poor cycle life and the need for pure oxygen.[6,7]

Typical Li-O_2 cells comprise a Li metal negative electrode (anode), an aprotic electrolyte and a porous positive electrode (cathode) mainly based on carbon materials. Common solvents are dimethyl sulfoxide (DMSO)[8] and ethers like monoglyme, diglyme or tetraglyme.[9] Because of a lack of appropriate filter systems for water and carbon dioxide pure oxygen is currently used in the cathode chamber instead of ambient air.[6,7] During discharge oxygen is reduced to form insoluble polycrystalline lithium peroxide (Li_2O_2) on the surface of the cathode.[10] Lithium superoxide (LiO_2) has been identified as an important intermediate by surface enhanced Raman spectroscopy (SERS).[11] The oxidation of the insoluble and poorly conducting Li_2O_2 requires a high overvoltage during the charging process and leads to a low round-trip efficiency.[12] Ottakam Thotiyl et al. identified the carbon cathode as a center of parasitic reactions during charging, including the oxidative decomposition of the cathode at high potentials.[13] The blocking of the carbon surface by decomposition products is considered as the major reason for the poor cycle life of Li-O_2 batteries.[14] Hence, the reduction of the overvoltage upon charging is the key step in the further development of Li-O_2 batteries, providing not only a higher efficiency but also a better cycling stability. Until now this strategy was mainly pursued by the use of heterogeneous catalysts like metal nanoparticles,[15,16] metal nitrides,[17] and also various classes of metal oxides.[18−20]

An alternative approach comprises dissolved redox mediators (RM), which act as mobile charge carriers between the electrode surface and Li_2O_2.[21] The charge transfer is based on the reversible redox pair RM ⇌ RM^+ + e^-. While heterogeneous catalysts influence the oxygen evolution reaction (OER) only at the limited and rigid contact surface to the depleting Li_2O_2, dissolved redox mediators provide oxidative attack at the much larger and dynamic interphase between Li_2O_2 and the liquid electrolyte.

Up to now two possible redox mediators have been investigated extensively in Li-O_2 cells, while additional redox

Received: August 16, 2014
Published: September 25, 2014

   dx.doi.org/10.1021/ja508400m | J. Am. Chem. Soc. 2014, 136, 15054−15064

couples were proposed in patent applications.[21,22] Chen et al. introduced a solution of tetrathiafulvalene (TTF) in DMSO using a nanoporous gold cathode.[23] Lim et al. combined lithium iodide (LiI) in tetraglyme with porous carbon nanotube fibrils.[24] Herein we propose the chemical class of nitroxides as dissolved redox mediators with very favorable properties for the OER in Li-O_2 cells. We investigated TEMPO (2,2,6,6-tetramethylpiperidinyloxyl) exemplarily, and the efficiency might be further improved by using other nitroxide compounds.

TEMPO is a persistent radical, which is sterically protected by four α-methyl groups. The reversible one electron oxidation leads to $TEMPO^+$, the corresponding N-oxoammonium cation (Scheme 1). TEMPO and its derivatives are commonly used as

Scheme 1. Redox Couple $TEMPO^+$/TEMPO.

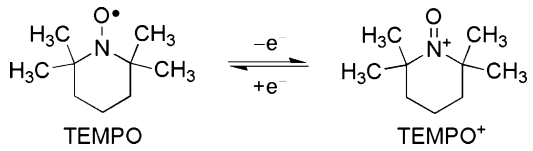

catalysts in organic reactions,[25−27] as agents for molecular weight control in polymerization processes[28,29] and as scavengers of protein radicals to prevent oxidative cellular damage.[30] Furthermore, TEMPO was shown to be an appropriate redox shuttle additive for overcharge protection in Li-ion cells.[31] Parallel to our work Hase et al. proposed the use of TEMPO as an indicator for the quantification of Li_2O_2.[32]

2. EXPERIMENTAL METHODS

Chemicals and Analytical Methods. Diglyme (Sigma-Aldrich, 99.5%) was distilled and dried over activated 3 Å molecular sieves for one week. LiTFSI (Sigma-Aldrich, 99.95%) was dried at 160 °C with a Büchi oven under a vacuum for 12 h. Solvent and salt had a final water content of ≤5 ppm determined by Karl Fischer titration (Mettler-Toledo). TEMPO (Sigma-Aldrich, 99%) and TTF (Sigma-Aldrich, 97%) were purified by sublimation, LiI (Sigma-Aldrich, 99.999%) was used as received. Powder X-ray diffraction (XRD) was carried out with an X'Pert Pro diffractometer from PANalytical (Cu Kα source, 40 kV, 40 mA) using a gastight sample holder. To detect possible degradation products the cathodes were rinsed with diglyme, dried in vacuo and subsequently investigated by Raman spectroscopy or ^{1}H NMR spectroscopy. The Raman spectra were recorded on a Senterra Raman microscope (Bruker, 633 nm excitation wavelength) using a gastight Linkam THMS600 cell. For the ^{1}H NMR analysis the cathodes were extracted with 1 mL D_2O and the extracted solutions were characterized using an Avance II 400 MHz or Avance II 200 MHz (both Bruker). All pressure data were recorded using a PAA-33X absolute pressure sensor, a K104B USB computer adapter, and the software Read30 v2.10 (all from Omega Engineering). The volumes of the different gas reservoirs were determined by parallel use of the pressure sensor and a calibrated syringe (Hamilton). The oxygen consumption and the gas evolution were calculated from the recorded pressure data on the basis of the ideal gas law. For the DEMS (differential electrochemical mass spectrometry) experiments we used a PrismaPlus QMG 220 M1 quadrupole mass spectrometer (Pfeiffer Vacuum) and a modified design of the presented Swagelok cells. Herein, a capillary was placed just above the cathode and the evolved gases were flushed out of the cathode chamber using helium as carrier gas. Pressure data, DEMS data and XRD patterns were smoothed using the Savitzky-Golay method without changing the basic form or suppressing relevant signals.

Cyclic Voltammetry (CV) and Chronoamperometry (CA). Cyclic voltammetry experiments were performed in an airtight three electrode cell (5 mL electrolyte) using Li^+/Li as reference electrode, platinum as the counter electrode and a glassy carbon working electrode (6 mm diameter). Prior to each experiment the glassy carbon electrode was carefully polished with a diamond slurry and an alumina slurry. After assembling the cells in an Ar filled glovebox the CV experiments were performed in Ar or O_2 atmosphere using a VMP3 or a SP300 potentiostat/galvanostat (BioLogic Science Instruments). Prior to the oxygen experiments pure O_2 was bubbled through the cell via an additional valve for five minutes. CV experiments were performed using either a 10 mM solution of TEMPO in 1 M LiTFSI/diglyme (to fully suppress an *IR* drop between working electrode and reference electrode) or the original battery electrolyte (10 mM TEMPO in 0.1 M LiTFSI/diglyme) for qualitative investigations only. The chronoamperometric experiments were conducted with the same setup using a SP300 potentiostat/galvanostat as well. Different potentials in the range from 4.1 V to 4.3 V were applied to the glassy carbon electrode and the corresponding current flow was monitored. An exemplary measurement is provided in Figure S3, Supporting Information (SI).

Oxygen Solubility. For the determination of the oxygen solubility approximately 5 mL carefully degassed electrolyte were placed in a glass flask (12 mL). A stainless steel cross fitting (Swagelok), which was connected to a pressure sensor, an oxygen reservoir and a vacuum pump by a manual ball valve (Swagelok), was mounted on the flask. Pure O_2 with a defined partial pressure was supplied in the flask and the subsequent pressure decrease corresponding to the oxygen absorption was monitored by the pressure sensor. Vigorous stirring ensured equilibrium concentrations after oxygen supply. For the determination of H_{O_2} (Henry constant) the experiment was repeated for several times at increasing oxygen partial pressures. An exemplary measurement is provided in Figure S4, SI.

Cycling of the Li-O_2 Cells. The galvanostatic measurements were performed in Swagelok-type cells containing a lithium metal anode, a lithium metal reference electrode (both from Rockwood Lithium), a porous carbon cathode, a glass fiber separator (Whatman), stainless steel current collectors and an airtight gas chamber (~7.2 mL). Lithium anodes were stored in a 0.1 M solution of LiTFSI in propylene carbonate (PC) for at least one week and thoroughly washed with diglyme prior to the assembling. For the manufacturing of the carbon cathodes a slurry of 75 wt % Ketjenblack EC600JD (AkzoNobel) and 25 wt % PTFE (polytetrafluoroethylene) was cast on a glass fiber separator (10 mm diameter). The investigated cells comprised approximately 0.3−0.5 mg of carbon in the cathodes and 60 μL of a 0.1 M LiTFSI/diglyme electrolyte either with 10 mM TEMPO or without TEMPO. One additional experiment was performed with a gas diffusion layer (GDL) cathode (Freudenberg H2315, Quintech, 10 mm diameter). The electrochemical cells were assembled in an Ar filled glovebox. After purging the gas chamber with oxygen (≈1 bar) galvanostatic measurements were performed using a Maccor battery cycler. During our experiments we did not observe any problems regarding a drying out of the cathode or the separator in the well sealed cell. Further details on the design of the cells are provided in the SI of a previous manuscript.[33] The specific capacity was based on the carbon mass of the cathode and the current density was calculated with the geometric area of the cathode. For the determination of the lifetime only cycles with final discharge voltages over 2.4 V were considered.

Confirmation of the Charging Mechanism. For the confirmation of the charging mechanism a slightly different setup was chosen to enable a flexible assembling, short diffusion paths and a fast start of the pressure monitoring. We used stainless steel current collectors, a lithium iron phosphate (LFP) based anode (84 wt % LFP, 8 wt % PVDF, 4 wt % carbon black, 4 wt % graphite, 12 mm diameter), a lithium reference electrode (Rockwood Lithium) and a carbon electrode consisting of a Ketjenblack film (same preparation as for the regular Li-O_2 cells) on a GDL (Freudenberg H2315, Quintech, 8 mm diameter). Anode and carbon electrode were separated by two pieces of a polypropylene (PP) membrane (Celgard 2400) containing 20 μL of a 0.1 M LiTFSI/diglyme electrolyte either with 100 mM TEMPO or without TEMPO. During discharge to 2.5 V (j = 0.1 mA

cm^{-2}) the carbon electrode was used as cathode provided by a direct electric contact to the current collector. Prior to the charging the carbon electrode was separated from the current collector by two pieces of the PP membrane soaked with another 20 μL of the electrolyte. An additional GDL layer was placed on the current collector to increase the surface area. Subsequently, a potential of 3.84 V vs Li^+/Li was applied to the current collector and current respectively pressure were monitored.

3. RESULTS AND DISCUSSION

A suitable redox mediator in Li-O_2 batteries has to fulfill the following essential conditions: (a) sufficient solubility in Li-O_2 electrolytes, while the optimal concentration depends on cathode structure, electrolyte and current density; (b) electrochemical stability in the voltage range of Li-O_2 batteries; (c) chemical stability in the environment of Li-O_2 batteries, which provides reactive species like O_2, LiO_2, and Li_2O_2; (d) a higher redox potential than the potential for formation of Li_2O_2 (2.96 V vs Li^+/Li)[2]; (e) sufficient oxygen solubility in the electrolyte with RM additive; (f) fast diffusion kinetics to guarantee an appropriate support of charge carriers at high currents.

Basic Characterization of TEMPO. Prior to the cycling measurements, the crucial physical and chemical data for an application of TEMPO as redox mediator in Li-O_2 cell were determined. A 0.1 M solution of lithium bis-(trifluoromethylsulfonyl)imide (LiTFSI) in diglyme was chosen as electrolyte allowing TEMPO concentrations of more than 1.0 M. However, suitable RM concentrations for state of the art Li-O_2 batteries will be in the range from 10 mM to 100 mM.

Primarily the redox electrochemistry of TEMPO was studied by cyclic voltammetry (CV) using a three electrode setup with a glassy carbon working electrode. The CV experiments were performed with a 10 mM solution of TEMPO in 1 M LiTFSI/diglyme to fully suppress the *IR* drop between working electrode and reference electrode in the used setup. Additional experiments were conducted with the original battery electrolyte (10 mM solution of TEMPO in 0.1 M LiTFSI/diglyme) for qualitative CV investigations of the redox chemistry only, see Figure S1a,b (SI). We chose a voltage range from 2.0 V to 4.55 V, which enabled stable and reproducible voltammograms over many cycles. The upper voltage limit of 4.55 V leads to a complete removal of previously formed carbonates under oxygen atmosphere but is low enough to prevent a strong electrochemical degradation of the electrolyte.[13,32] The voltammogram under argon atmosphere (Figure 1a) showed a reversible electrochemical oxidation of TEMPO to $TEMPO^+$, since the ratio of cathodic peak current ($I_{p,c}$) and anodic peak current ($I_{p,a}$) is approximately 1 ($I_{p,c}/I_{p,a}$ = 0.99). The determination of the peak current is exemplarily shown in Figure S2 (SI). Furthermore, a formal potential of 3.74 V vs Li^+/Li was determined for the redox couple $TEMPO^+$/TEMPO in diglyme, which corresponds to the midpoint between cathodic and anodic peak.

An additional reduction step was observed at $U \leq 2.2$ V, which is related to the redox couple TEMPO/$TEMPO^-$.[35] A full scan of this redox step is shown in Figure S1b (SI). The corresponding oxidation peak is missing, and hence the reduction to $TEMPO^-$ in diglyme appears to be irreversible, which was already reported by Chabita for an aqueous solution.[36] As Li-O_2 cells usually exhibit a discharge plateau at around 2.7 V, the parasitic reduction of TEMPO at the cathodic side is considered to be very unlikely. The reversible electrochemical oxidation of TEMPO is also observed under

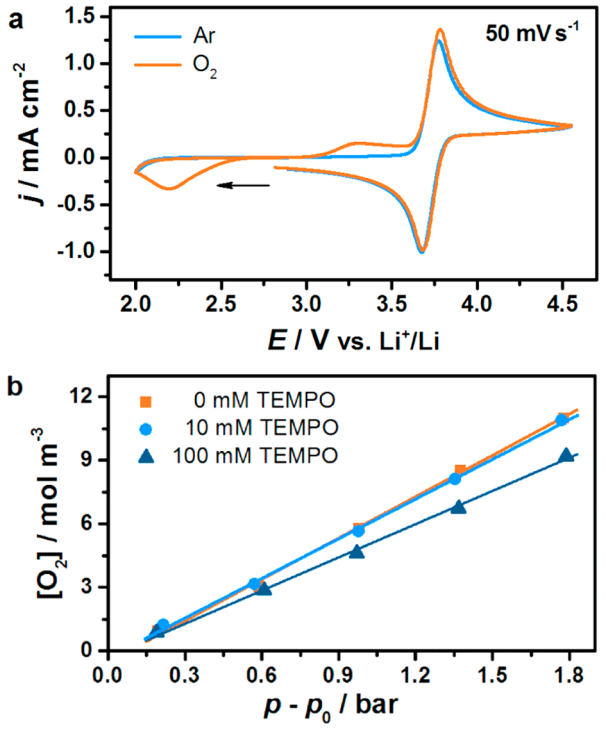

Figure 1. (a) Cyclic voltammogram of a 10 mM solution of TEMPO in 1 M LiTFSI/diglyme under Ar and O_2 atmosphere. (b) Pressure dependent O_2 concentrations of a 0.1 M LiTFSI/diglyme solution containing no TEMPO, 10 mM TEMPO and 100 mM TEMPO. An exemplary measurement for one of the five steps is shown in the Supporting Information (Figure S4, SI).

oxygen atmosphere including different reactive oxygen species during the CV cycle. This is indicated by a ratio of the peak currents $I_{p,c}/I_{p,a}$ = 0.99 as well. In summary, the stability of TEMPO under the condition of a Li-O_2 cell is confirmed by the CV data. The formal potential of 3.74 V is the prerequisite that the reversible chemical oxidation of Li_2O_2 by dissolved $TEMPO^+$ is possible.

To evaluate the diffusion kinetics of TEMPO, the diffusion coefficient D_T was determined for a 10 mM solution of TEMPO in 0.1 M LiTFSI/diglyme by chronoamperometry.[37] Herein, different potentials in the range of 4.1 V to 4.3 V were applied and the respective currents were detected corresponding to the electrochemical formation of $TEMPO^+$. The time dependent decrease of the current is described by the Cottrell equation:

$$|j| = zFD_T^{1/2}c_T(\pi t)^{-1/2} \quad (1)$$

where j is the current density, z is the electron number, F is the Faraday constant and t is the time. Further information and a data plot are provided in the Supporting Information (Figure S3, SI). A TEMPO diffusion coefficient of $1.4{\cdot}10^{-5}$ cm^2 s^{-1} (Table 1) was determined, which is only slightly lower than the diffusion coefficient of oxygen in pure diglyme ($D_{O_2} = 4.4{\cdot}10^{-5}$ cm^2 s^{-1}).[38] Chabita et al. determined a TEMPO diffusion coefficient of $1.5{\cdot}10^{-5}$ cm^2 s^{-1} for an aqueous solution by CV.[36] Since the diffusion kinetics is sufficiently fast, high TEMPO concentrations are not necessarily required for an application in Li-O_2 cells at moderate current densities.

For the determination of the optimal concentration the influence of TEMPO on the oxygen solubility (Henry constant,

dx.doi.org/10.1021/ja508400m | J. Am. Chem. Soc. 2014, 136, 15054−15064

Table 1. Oxygen Solubility (H_{O_2}) and TEMPO Diffusion Coefficient (D_T) of a 0.1 M LiTFSI/Diglyme Solution with Different TEMPO Concentrations.

[TEMPO]/mmol L^{-1}	H_{O_2}/mol $(m^3 \cdot bar)^{-1}$	$D_T/10^{-5}$ cm^2 s^{-1}
0	6.6 ± 0.1[a]	
10	6.5 ± 0.3[a]	1.4 ± 0.2[a]
100	5.2 ± 0.2[a]	

[a]Average value of at least two independent measurements

H_{O_2}) of a 0.1 M LiTFSI/diglyme solution was measured, using a method adopted from Camper and Hartmann.[38] This method is based on the pressure monitoring of an oxygen reservoir during absorption in a previously degassed electrolyte. For the calculation of H_{O_2} the oxygen solubility was determined at different partial pressures.

Table 1 shows a clear correspondence between TEMPO concentration and oxygen solubility. Addition of 100 mM TEMPO to the electrolyte leads to a decrease of the oxygen solubility from 6.6 mol m^{-3} (6.6 mM) at 1 bar to 5.2 mol m^{-3} (5.2 mM) at 1 bar, indicating a slight salting out effect of TEMPO on oxygen. However, a 10 mM TEMPO solution still showed an oxygen solubility of 6.5 mol m^{-3} (6.5 mM) at 1 bar, supporting the use of 10 mM TEMPO as the reference catalyst concentration in the electrochemical experiments. We note that the Henry constant of the 0.1 M LiTFSI/diglyme electrolyte

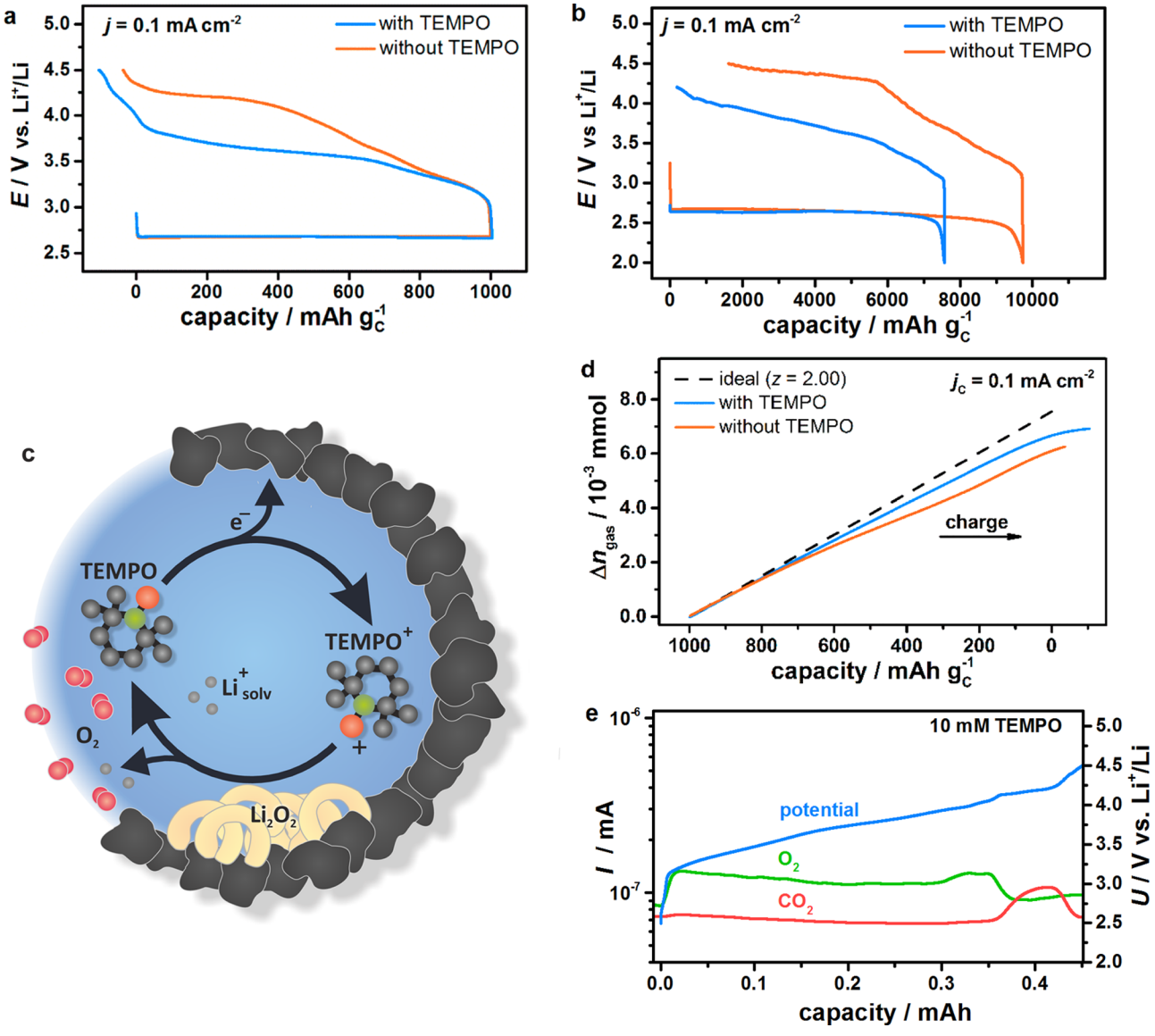

Figure 2. (a) First cycle with and without 10 mM TEMPO using a Ketjenblack cathode and a constant current density of 0.1 mA cm^{-2}. (b) Full cycle of a Li-O_2 cell with and without 10 mM TEMPO using the same conditions like (a). Both cells were discharged to 2.0 V, the cell without TEMPO was charged to 4.5 V, whereas the cell with TEMPO was only charged to 4.2 V due to the lower charging overpotentials. (c) Proposed catalytic cycle for the electrochemical charging of Li-O_2 cells with TEMPO. (d) Gas evolution on the basis of the recorded cell pressure during the first charge of the cells shown in (a). The black line corresponds to an ideal oxidation of Li_2O_2 with a z value ($n(e^-)/n_{gas}$) of 2.00. Uncertainty of Δn_{gas} after full charge is 5.2% (without TEMPO) and 4.4% (with TEMPO). (e) Differential electrochemical mass spectrometry (DEMS) analysis of the evolved gases during the charge of a Li-O_2 cell with 10 mM TEMPO (j = 0.1 mA cm^{-2}). The left axis represents the detected ion currents of the selected m/z ratios for the species O_2 (32) and CO_2 (44), the right axis shows the voltage profile of the charging step.

dx.doi.org/10.1021/ja508400m | J. Am. Chem. Soc. 2014, 136, 15054−15064

(H_{O_2} = 6.6 mol m^{-3} at 1 bar) is in good agreement with the corresponding data of pure diglyme published by Hartmann et al. (H_{O_2} = 6.4 mol m^{-3} at 1 bar).[38]

TEMPO in Li-O_2 Cells. A common setup, based on a Swagelok design with a fully sealed gas reservoir,[33] was chosen for the Li-O_2 cells to enable a high reproducibility. We used a lithium anode, a lithium reference electrode and a porous cathode consisting of commonly used Ketjenblack and PTFE as binder. The anode was pretreated with a 0.1 M solution of LiTFSI in propylene carbonate to stabilize the lithium metal[8] and to minimize an irreversible reduction of TEMPO at the negative electrode. However, a practical application of Li-O_2 batteries will require a more rigid protective layer on the lithium anode, at least to prevent the reduction of oxygen at the lithium metal surface.[39] At first, Li-O_2 cells with and without 10 mM TEMPO were cycled under 1 bar of oxygen at a current density of 0.1 mA cm^{-2}. The two model cells were discharged to a specific capacity of 1000 mAh g_C^{-1} and subsequently charged to a voltage limit of 4.5 V. As illustrated in Figure 2a, the discharge plateau of approximately 2.7 V is not influenced by the addition of TEMPO. This provides evidence that the electrochemical reduction of oxygen to superoxide at the cathode surface is not affected by TEMPO. To further investigate the influence of TEMPO on the discharge processes and especially on the maximal capacity similar cells with and without TEMPO were discharged to 2.0 V. As illustrated in Figure 2b TEMPO reduces the maximal discharge capacity of the corresponding Li-O_2 cells from 9700 mAh g_C^{-1} (without TEMPO) to 7400 mAh g_C^{-1} (with 10 mM TEMPO). This provides evidence that the second reduction step from superoxide to Li_2O_2 might be influenced by TEMPO. For this reaction either a second electrochemical step or/and a chemical disproportionation of superoxide are discussed.[11,34,40] Adams et al. proposed a significant contribution of the solution phase to the second reduction step,[40] which is in accordance with the elucidated influence of the dissolved TEMPO on the formation of Li_2O_2.

For a further investigation of the discharge reaction the cell pressure of the model cells with a fixed capacity of 1000 mAh g_C^{-1} was monitored by a pressure sensor.[38] This offers direct information on the link between electrochemical charge transfer and consumption of oxygen. The discharge of both, a Li-O_2 cell with and without TEMPO, led to a linear decrease of the pressure. The corresponding quantity of oxygen was calculated (Figure S5, SI) and the ratio of electrons per gas molecule ($n(e^-)/n_{gas}$), the charge number z, was determined. Herein, z values of 2.01 ± 0.08 (with TEMPO) and 2.02 ± 0.09 (without TEMPO) were obtained fitting well with an ideal two-electron reduction to form Li_2O_2. These data are well in line with the results of McCloskey et al., who determined a value of $z \approx 2$ for different carbon materials.[41] The predominant formation of Li_2O_2 in cells with TEMPO was further confirmed by XRD showing no reflections of other crystalline materials (Figure 3).

However, even in Li-O_2 cells with comparably stable ether based electrolytes a minor fraction of decomposition products like lithium carbonate, lithium formate and lithium acetate is formed during discharge.[42] These species are not apparent in XRD but could be detected by ^{1}H NMR spectroscopy,[43] IR spectroscopy[43] or Raman spectroscopy.[44]To clarify the formation of decomposition products discharged cathodes of Li-O_2 cells with and without 10 mM TEMPO were investigated

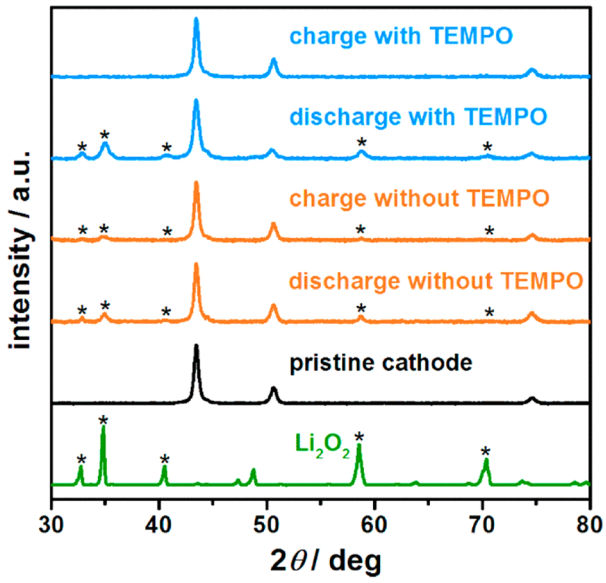

Figure 3. XRD pattern of the cathode after discharge to 2.5 V and subsequent charge to 4.15 V, each with a current density of 0.1 mA cm^{-2}. Li-O_2 cells with a Ketjenblack cathode were cycled under O_2 atmosphere using a 0.1 M LiTFSI/diglyme electrolyte that contained 10 mM TEMPO (blue) or no TEMPO (red).

by Raman spectroscopy. As shown in Figure S6 (SI), only the peaks of diglyme, LiTFSI and Li_2O_2 could be clearly identified for both cells. The corresponding signature of Li_2CO_3 is not detected by Raman spectroscopy. This indicates that the formation of lithium carbonate does not contribute significantly to the discharge chemistry (compared to Li_2O_2 formation). However, we expect lithium carbonate to be formed in minor amounts during discharge as reported in several detailed investigations of reactions in ether based Li-O_2 cells.[13,42] The formation of lithium formate and lithium acetate cannot be evidenced by Raman spectroscopy since both species only show peaks of minor intensity in the selection region of the spectrum. To detect these species discharged cathodes were extracted with D_2O and the solutions were subsequently investigated by ^{1}H NMR spectroscopy, see Figure S7 (SI). The spectrum of the cell with TEMPO shows the same peaks like the corresponding cell without TEMPO, which provides evidence that TEMPO does not facilitate additional degradation reactions. Both spectra are in good agreement with the data reported by Freunberger et al. for ether based electrolyes[42] and mainly show the presence of formic acid, acetic acid and residual diglyme (formic acid and acetic acid are formed by the reaction of lithium formate/lithium acetate and D_2O).[43] A direct comparison of both spectra demonstrates an increased formation of lithium acetate in the presence of TEMPO, which indicates that TEMPO particularly promotes the formation of lithium acetate during discharge. However, further research on stable electrolytes and cathode materials might overcome this problem in the future.

As expected due to the CV data, the charging voltage is significantly reduced in the presence of TEMPO leading to a distinct improvement of the round-trip efficiency. Likewise, a small overcharge of about 100 mAh g_C^{-1} was observed. In detail, the cell with TEMPO provided a plateau-like charging curve, mostly below 3.7 V. This fits with the catalytic concept of dissolved redox mediators, which is schematically illustrated in Figure 2c. The proposed catalytic cycle comprises of two parts:

dx.doi.org/10.1021/ja508400m | J. Am. Chem. Soc. 2014, 136, 15054−15064

(1) Diffusion of TEMPO to the carbon surface and subsequent electrochemical oxidation to $TEMPO^+$. (2) Diffusion of $TEMPO^+$ to Li_2O_2 and chemical oxidation of Li_2O_2 by $TEMPO^+$. Since the oxidation of TEMPO to $TEMPO^+$ represents the only electrochemical step in the cycle, the observed charging profile is solely governed by this process. As a result the charging potential is predominantly determined by the redox potential of the nitroxide species. A minor contribution is also provided by the electrode kinetics and diffusion. On the basis of this analysis we expect the charging plateau from 3.5 V−3.7 V to correspond to the electrochemical oxidation of TEMPO to $TEMPO^+$. This is supported by the corresponding CV (Figure 1a), which showed an increase of the oxidative current slightly above 3.5 V. Nevertheless, the formation of $TEMPO^+$ does not necessarily lead to the favored catalysis of the oxygen evolution reaction (OER). The subsequent oxidation of lithium peroxide to oxygen has to be proven by additional experiments since a short circuit shuttle to the anode might be a competing reaction. A similar phenomenon is known from Li-S batteries[45,46] and is associated with a parasitic overcharge. Nonetheless, compared to the total capacity of the first cycles, we expect only a minor contribution of a parasitic shuttle for the following reasons: $TEMPO^+$ is predominantly formed at the large pore surface of the carbon cathode and in direct vicinity of Li_2O_2. Hence, we assume that $TEMPO^+$ is instantaneously consumed by adjacent Li_2O_2 before significant diffusion to the anode is initiated. A first indication of a negligible anode shuttle is the strong increase of the voltage in the charging profile when the discharge capacity is met. This is also known from other rechargeable battery systems and indicates the depletion of rechargeable material (discharge products),[47] in this case Li_2O_2.

Further evidence was provided by monitoring the cell pressure. Figure 2d illustrates the corresponding gas evolution during the charge in Li-O_2 cells with and without TEMPO. Analogous to the discharge the ideal and exclusive oxidation of Li_2O_2 was considered as a benchmark characterized by a constant gas evolution with z = 2.00 (dashed line). Cells without TEMPO matched this ideal behavior solely at the beginning of the charging step. After charging to a capacity of around 200 mAh g_C^{-1} the formation rate of gas decreased drastically resulting in a significant deviation from the oxidation of Li_2O_2. This deviation provides clear evidence of competitive decomposition reactions, which lead to the formation of solid products like carbonates, acetates or formates.[41] In contrast, the charging of Li-O_2 cells with TEMPO showed a distinctly stronger gas evolution leading to better consistency with the ideal Li_2O_2 oxidation.

However, the detected gas evolution does not necessarily indicate the evolution of oxygen during the charging process, since the parallel formation of other gaseous species is reported for Li-O_2 cells.[13,41] Ottakam Thotiyl et al. reported the evolution of CO_2 in ether based Li-O_2 cells even at voltages above ∼3.2 V mainly originating from the oxidation of the decomposition products of the discharge step.[13] The degradation of the electrolyte and the carbon cathode during charging leads to the continuous formation of CO_2 above 3.5 V. McCloskey et al. investigated the charging step of Li-O_2 cell by DEMS (differential electrochemical mass spectrometry) using an ether based electrolyte as well and a P50 carbon paper as cathode.[41] Oxygen formation contributed mainly to the gas evolution during the charging step (29.5 μmol, 86%), while CO_2 (3.4 μmol, 10%) and H_2 (1.3 μmol, 4%) were evolved in minor amounts. The highest oxygen evolution rate was detected during the initial step of the charging process, corresponding to a voltage raise mainly below 4.0 V. During the charging at voltages >4.0 V the formation rate of oxygen was significantly lower than expected for oxidation of Li_2O_2. As the Li-O_2 cells with TEMPO exhibit a charging plateau distinctly below 4.0 V (Figure 2a), a higher relative yield of oxygen (% O_2) is expected compared to common Li-O_2 with a charging plateau above 4.0 V. To further investigate the charging process in the presence of TEMPO the evolved gas species were analyzed by DEMS (Figure 2e). We focused on CO_2 as main decomposition product and oxygen, which were detected in situ using a quadrupole mass spectrometer and a constant flow of helium as carrier gas. The charging profile under these conditions differs slightly from the profile of the corresponding cell with a closed O_2 reservoir and shows a stronger contribution of the second charging plateau at ∼4.2 V. Parallel to the beginning of the charging step at 0 mAh a strong increase of the ion current for the m/z value of oxygen (32) is observed accompanied by a minor increase of the ion current for the m/z value of CO_2 (44). While the signal of CO_2 suddenly decreases to zero, a strong evolution of oxygen is detected during the whole charging plateau below 4.0 V. The oxygen signal severely decreases exactly at the transition of the first charging plateau to the second charging plateau above 4.0 V. Concurrently, the formation of CO_2 steeply raises and CO_2 remains the major contributor to the total gas evolution during the whole plateau. These results provide clear evidence that the use of TEMPO enables a separation of the favored OER (first plateau) from degradation reactions and the subsequent oxidation of these species to CO_2 (second plateau). In regular Li-O_2 cells both reactions occur essentially parallel during the high charging voltages.[41]

In view of the higher pressure increase in the presence of TEMPO with the predominant formation of oxygen during the first charging plateau, we can unequivocally prove an improved efficiency of the charging reaction by TEMPO. The improved efficiency is mainly attributed to the high mobility of TEMPO. Dissolved species are able to oxidize large Li_2O_2 particles with an extremely low electric conductivity. Even Li_2O_2 formed on the separator could be oxidized by mobile $TEMPO^+$, which would be impossible in a common cell due to the lack of an electric contact. A further discussion about the mechanism is given in the following section. The consistency between gas evolution (Figure 2d) and charging current (Figure 2a) confirms the mainly catalytic shuttle of TEMPO during the first charge. The z value of 2.20 ± 0.10 indicates small contributions from side reactions including primarily degradation reactions[41] and from the parasitic shuttle to the anode. It should be pointed out that only the recharge of the discharge capacity (1000 mAh g_C^{-1}) led to a significant gas evolution in Li-O_2 cells with TEMPO (Figure 2a,d).

An additional comparison of the charging efficiency with and without TEMPO is provided by XRD analysis of cathodes after one complete cycle (Figure 3). Here, Li-O_2 cells were discharged to 2.5 V and subsequently charged to a voltage of 4.15 V, which is slightly below the high voltage plateau of the cells without TEMPO (Figure 2a). While Li_2O_2 is still detectable after charging a cell without TEMPO, no diffraction patterns of Li_2O_2 were recorded using an electrolyte with TEMPO. This is in line with the presented pressure and cycling data, since cells with TEMPO showed neither a significant gas evolution nor a distinct charging step between 4.15 and 4.5 V.

The decrease of the charging overpotential by addition of 10 mM TEMPO is not only provided at a discharge capacity of 1000 mAh g_C^{-1} but also after full discharge. In this case, the voltage of a Li-O_2 cell with TEMPO is reduced by around 600 mV during the whole charging process compared to the corresponding cell without TEMPO, see Figure 2b.

In the following the influence of the charging current magnitude on the cycling performance of Li-O_2 cells with and without TEMPO is discussed. Since the discharge current has a distinct influence on the formation of Li_2O_2,[40] the current was kept constant during discharge for all experiments. This enables a direct comparison of the more relevant charging reactions at different current densities. As illustrated in Figure 4a and Figure

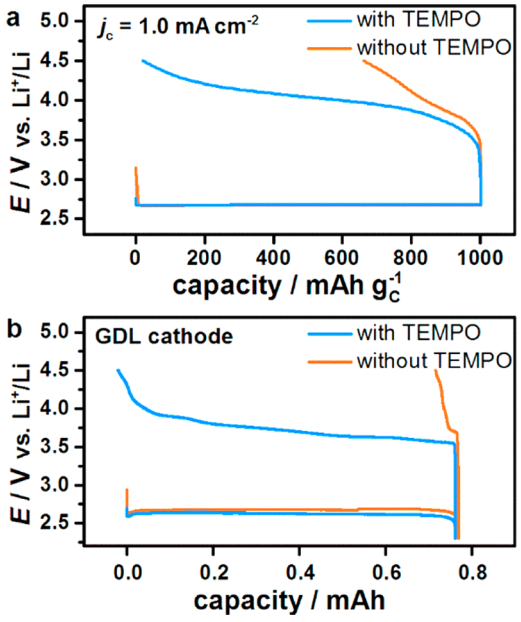

Figure 4. First cycle with and without TEMPO using a discharge current density of 0.1 mA cm^{-2}, (a) a Ketjenblack cathode and a charge current density of 1.0 mA cm^{-2}, (b) a GDL cathode and a charge current density of 0.1 mA cm^{-2}.

S8 (SI), higher charging currents led to distinct increase of the overvoltage and a minor rechargeability in Li-O_2 cells without TEMPO. For example, only 1/3 of the discharge capacity could be recharged with 1.0 mA cm^{-2}. In case of Li-O_2 cells with TEMPO, full charge was possible, even at charging current densities of up to 1.0 mA cm^{-2}. Nevertheless, an increase of the charging overvoltage was observed as well, probably attributed to current dependent limitations of the diffusion and electrode kinetics. The catalytic effect is even more pronounced when using cathode materials of low specific surface area, exemplarily shown for a gas diffusion layer (GDL) in Figure 4b. While usual Li-O_2 cells with GDL cathodes could not be charged at a moderate current density of 0.1 mA cm^{-2}, the addition of 10 mM TEMPO led to a complete electrochemical charging at the same conditions.

The use of mobile redox mediator leads to the additional question whether a self-discharge of Li-O_2 cells might be supported. In this case the charge transfer would have to be based on the couple TEMPO/TEMPO$^-$, which provides a lower redox potential than the formation of Li_2O_2, see Figure S1 (SI). However, we do not expect a major influence of such a self-discharge shuttle since the formation of TEMPO$^-$ is irreversible and also minimized by pretreating the anode with propylene carbonate.[8] To confirm this a Li-O_2 cell with 10 mM TEMPO was stored for 24 h at open circuit voltage (OCV) and was subsequently analyzed by XRD. As illustrated in Figure 5 no evidence for the formation of Li_2O_2 could be observed.

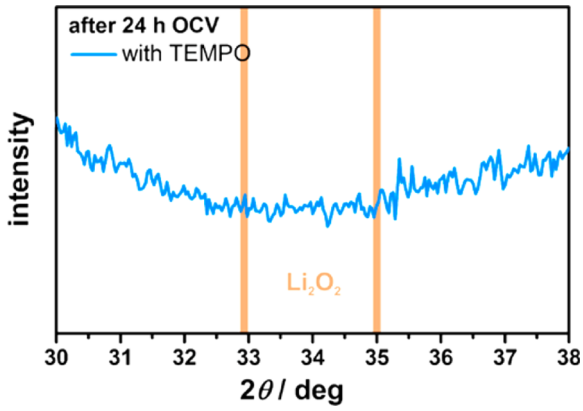

Figure 5. XRD pattern of a Ketjen Black cathode after 24 h of open circuit voltage (OCV) in a Li-O_2 with 10 mM TEMPO under O_2 atmosphere. Reflexes of Li_2O_2 are centered at 32.9 and 35.0°, compare Figure 3.

Finally we investigated the cycle stability of Li-O_2 cells with and without TEMPO at a fixed capacity of 500 mAh g_C^{-1} for discharge and charge. A fixed charge capacity is expected to minimize the contribution of parasitic degradation reactions, since only a minor gas evolution was detected during the overcharging of TEMPO containing cells in the first cycle. A voltage criterion will also be unfavorable since degradation reactions lead to electrode passivation and an increasing polarization during cycling.[13] Without TEMPO we only obtained 27 stable cycles (Figures 6a and S9a, SI) mainly based on the accumulation of degradation products on the cathode surface.[42] In contrast, over 55 stable cycles were achieved using an electrolyte with TEMPO. The cycles 1, 10, 25, 50 are exemplarily shown in Figure 6b, further details are provided in Figure S9b, SI. The improved lifetime of cells with TEMPO is mainly attributed to the lower charging voltages, which provide a significantly lower influence of the parasitic degradation reactions during charging.[13]

However, an increase of the charging voltage at higher cycle numbers is even observed for the Li-O_2 cell with TEMPO. We account the increasing coverage of the electrode surface with decomposition products as the major reason for the rise of the charging voltage. The successive accumulation of degradation products (e.g., lithium carbonate) during cycling was reported for ether based Li-O_2 cells in various studies.[42,13] McCloskey et al. calculated that even two monolayers of lithium carbonate significantly reduce the exchange current density of any electrochemical reaction, which depends on a charge transfer through the carbon electrode.[14] Compared to the cell without TEMPO (Figure 6a) the cycling of the Li-O_2 cells with TEMPO show a small but beneficial decrease of the discharge overpotentials during the first 25 cycles (Figure 6b). This is either attributed to a direct influence of TEMPO on the discharge chemistry, as already shown by the decreased capacity during the first cycle (Figure 2b), or it is due to the change of the oxidation chemistry during the previous charge. The efficient oxidation of Li_2O_2 during the charge with TEMPO

dx.doi.org/10.1021/ja508400m | J. Am. Chem. Soc. 2014, 136, 15054−15064

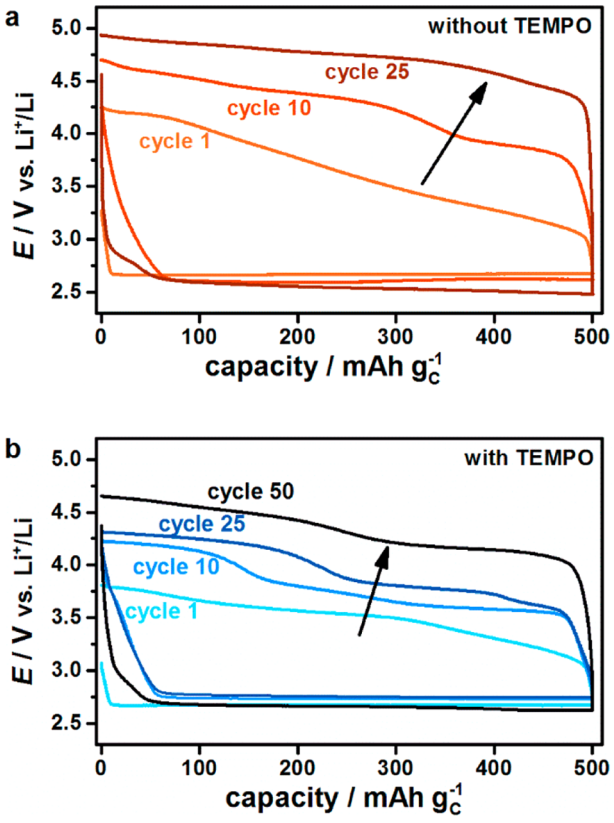

Figure 6. Cycling stability of a Li-O_2 cell (a) without and (b) with 10 mM TEMPO at a current density of 0.1 mA cm^{-2} using a Ketjenblack cathode and a 0.1 M LiTSFI/diglyme electrolyte under O_2 atmosphere.

might facilitate the O_2 reduction and Li_2O_2 formation in the subsequent discharge. The cycling of the Li-O_2 cell with TEMPO shows two separate cycling plateaus (Figure 6b): The first cycles are mainly characterized by the low charging plateau, while the higher plateau increases its contribution to the total charge capacity with higher cycle number. Finally the high charging plateau accounts for ~50% of the charge capacity during the 50th cycle. The two charging plateaus of the cycling profile (Figure 6b) fit well with the charging profile of Figure 2e showing two separate charging plateaus at the same voltages as well. We suggest that the low charging plateau of the cycling profile corresponds to the TEMPO catalyzed oxidation of Li_2O_2, since a parallel formation of O_2 was detected for the corresponding plateau in Figure 2e by DEMS. The decomposition reactions and the subsequent oxidation of these products are expected to occur mainly at the second plateau due to the evolution of CO_2 at the corresponding plateau in Figure 2e. On the basis of this hypothesis the increasing contribution of the second plateau fits well with the accumulation of degradation products during cycling.[13,42]

Since Li_2O_2 seems to be fully charged after the first plateau, we expected TEMPO to be fully oxidized after charging at the high voltages of the second plateau. This should then lead to a small reduction plateau of $TEMPO^+$ at the beginning of the subsequent discharge showing a maximal theoretical capacity of around 30 mAh g_C^{-1} and overpotentials comparable to those of the previous oxidation of TEMPO. The missing of this reduction plateau may be originated in a direct reduction of $TEMPO^+$ by intermediates of the decomposition reactions at the high voltage plateau. Furthermore, this might also indicate that the $TEMPO^+$ reduction could not account for the complete electrochemical charge transfer at the applied discharge current due to unfavorable and long diffusion paths after the long charging period. The latter case would lead to a parallel reduction of $TEMPO^+$ and oxygen even at the beginning of the discharge and hence to a mixed potential of both reaction, which then explains that no pronounced reduction plateau of $TEMPO^+$ is observed.

However, the first decomposition reactions already start at an even low charging potential of 3.5 V.[13] Hence, a chemical modification of TEMPO will be beneficial to further decrease the charging voltages by using substituents with a positive inductive or mesomeric effect. And in contrast to the majority of heterogeneous catalysts, it will be easier to tailor the redox properties of an organic redox mediator by molecular design/engineering. Hodgson et al. presented a systematic study on the redox properties of various nitroxides using ab inito calculations.[35] Their results indicate that azaphenale derivatives may be promising candidates since their oxidation potential in water is up to 300 mV lower than the corresponding potential of TEMPO.

To be able to assess the catalytic performance of TEMPO, identical cells with 10 mM LiI and 10 mM TTF as catalysts were assembled, following the work by Lim et al.[24] and Chen et al.[23] We consider LiI and TTF as a reasonable benchmark, since both compounds were already used as redox mediators in Li-O_2 cells.[24,23] We would like to add that Sun et al. have also recently proposed the use of iron phthalocyanine.[48] During the first cycle both, LiI and TTF, showed a superior cycle performance compared to TEMPO (Figures S10 and S11, SI). However, a strong increase of the charging voltages was observed at the subsequent cycles exceeding the overpotentials of the Li-O_2 cell with TEMPO. Finally, both catalysts did not provide an improvement of the cycle life compared to the cell without additives: 27 stable cycles were obtained with TTF, only 20 cycles were achieved with LiI. Both results highlight the stability and prospect of TEMPO and TEMPO-derivatives based catalysis in the presented Li-O_2 system. This cell system with a high capacity carbon cathode and a diglyme based electrolyte as one representative of the widely used class of ether electrolytes can be considered as a model system for Li-O_2 cells. However, we would like to emphasize that the interaction between solvent and dissolved redox mediator might have a distinct influence on the catalytic performance of the redox mediator. Hence, further research on this topic will require a parallel optimization of solvent, cathode and redox mediator.

Confirmation of the Charging Mechanism. The suggested mechanism for TEMPO mediated oxidation differs from the charging of a common Li-O_2 cell mainly in an additional charge transfer through the liquid electrolyte phase. Hence, it is expected that dissolved TEMPO enables the oxidation of previously formed Li_2O_2 without a direct electric contact to the current collector during charging. To address this hypothesis, Li-O_2 cells with and without TEMPO were discharged to 2.5 V and two sheets of separator soaked with electrolyte were subsequently placed between cathode and current collector. A TEMPO concentration of 100 mM was chosen due to the distinctly longer diffusion paths compared to the previous cycling experiments. Furthermore lithium iron phosphate (LFP) was used as anode material to enable an efficient conversion of TEMPO to $TEMPO^+$. Sufficient

dx.doi.org/10.1021/ja508400m | J. Am. Chem. Soc. 2014, 136, 15054−15064

formation of $TEMPO^+$ at the positive electrode was provided by applying a constant voltage of 3.84 V.

Figure 7 illustrates the corresponding current and cell pressure for the cells with and without TEMPO. The Li-O_2 cell

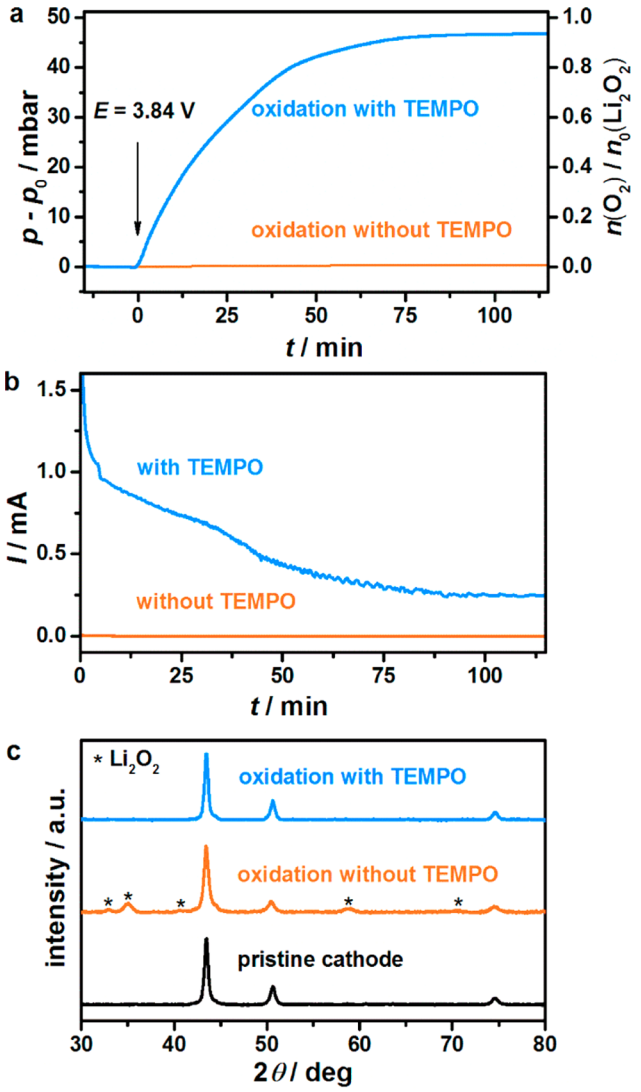

Figure 7. Monitoring of (a) cell pressure and (b) current during charge of a previously discharged carbon electrode at 3.84 V without direct electrical contact between carbon electrode and current collector. The experiments were conducted in Ar atmosphere using a 0.1 M LiTFSI/diglyme electrolyte with 10 mM TEMPO or without TEMPO. (c) XRD pattern after charging for 115 min.

without TEMPO showed neither a significant current nor a detectable gas evolution confirming that a direct flow of electrons is necessary for the oxidation of Li_2O_2 in a common Li-O_2 cell. However, in the presence of TEMPO a significant gas evolution and a distinct current were detected exactly after applying the voltage. The total pressure increase corresponds to an oxidation of 92% of the previously discharged oxygen assuming an exclusive evolution of oxygen during charging. This is in accordance with studies of Hase et al., who demonstrated that only 96% of the discharge capacity contributed to the formation of Li_2O_2 in a significantly more stable ionic liquid.[32]

The results were further supported by a XRD analysis of the cathodes after the oxidation experiment (Figure 7c). Significant intensity of Li_2O_2 reflexes was monitored using an electrolyte without TEMPO. No detectable quantities of Li_2O_2 were observed after applying the voltage in a cell with TEMPO. However, a comparison of current and pressure shows that the oxygen formation in the TEMPO containing cell corresponds to only ~2/3 of the measured charge transfer. This is a clear indication for a parallel (parasitic) shuttle to the anode, since the surplus of charges (0.32 mAh) exceeded the pure capacity of the dissolved TEMPO (0.11 mAh), according to the complete oxidation to $TEMPO^+$. On the basis of Fick's first law of diffusion the maximal (stationary) current for both, a catalytic shuttle to Li_2O_2 and parasitic shuttle to the anode, can by calculated by

$$j_{max} = \frac{D_T F c_T}{d} \quad (2)$$

In this equation j is the current density, D_T is the diffusion coefficient of TEMPO, c_T is the concentration of TEMPO and d is the distance between the areas of $TEMPO^+$ generation and consumption. It should be pointed out that eq 2 solely leads to an upper limit of the shuttle current due to two reasons: (a) The oxidation experiment (Figure 7) as well as most of galvanostatic charging were conducted at $E \leq 3.84$ V which is too low for a pure diffusion control of the shuttle current (according to a formal potential of 3.74 V). (b) Only half of the shuttle cycle corresponds to the diffusion of TEMPO, the other part is based on the (back) diffusion of $TEMPO^+$. We expect $TEMPO^+$ to diffuse slightly slower than TEMPO due to the positive charge. However, eq 2 can be used to estimate the contributions of the catalytic and the parasitic shuttle in the different experiments. Both shuttles only differ in the distance d between sites for $TEMPO^+$ formation and consumption. During galvanostatic cycling the maximal diffusion path d of the catalytic shuttle is expected to be in the range of the Li_2O_2 particle size (up to 500 nm),[40] while the distance to the anode is around 260 μm in our case (original thickness of the glass fiber separator). Assuming an identical cross-section area for both diffusion paths a ratio of catalytic current to parasitic current of at least ≈500:1 is calculated. In contrast, the abovementioned oxidation experiment provides a smaller difference between the competitive diffusion paths: around 50 μm are estimated for the distance between the current collector and Li_2O_2 (PP separators), 310 μm for the distance between current collector and anode (PP separators and carbon cathode). Hence the ratio of the catalytic shuttle to the parasitic shuttle is expected to be ≈6:1 (current densities) respectively ≈3:1 (total currents), taking into account the different geometric areas of the anode and the carbon electrode. The calculated ratio fits well with the detected current profile (Figure 7b) since a predominant catalytic shuttle is assumed during the strong gas evolution of the first 50 min and a purely parasitic shuttle is expected for the last 15 min. The confirmation of a parasitic shuttle to the anode clearly shows that an efficient use of redox mediators will require an optimized design of Li-O_2 cells including particularly the porous structure of the cathode.

4. CONCLUSION AND OUTLOOK

In conclusion, the proposed charging mechanism of a mobile redox mediator could be confirmed. We demonstrate that TEMPO is a highly suitable redox mediator for the OER in Li-

dx.doi.org/10.1021/ja508400m | J. Am. Chem. Soc. 2014, 136, 15054−15064

O_2 cells. TEMPO exhibits high electrochemical stability, fast diffusion kinetics, an appropriate redox potential and enables a sufficient oxygen solubility. The use of TEMPO in Li-O_2 cells leads to a significantly reduced charging voltage and, hence, to a distinctly higher round-trip efficiency. The observed charging plateau is associated with a parallel gas evolution indicating at most a minor contribution of a parasitic shuttle to the anode, which might be overcome by a proper cathode design. However, a parasitic shuttle was identified by changing the ratio of the competitive diffusion paths. Furthermore, TEMPO provides a significantly enhanced cycle life primarily based on the reduced charging voltages. The catalytic activity of TEMPO allows a wide range of current densities and different carbon based cathode materials. Since TEMPO is only one typical representative for the chemical class of nitroxides, modification of the chemical substituents may lead to a further decrease of the charging potential[35] and to an enhancement of the efficiency. Meanwhile, TEMPO was also used as a catalyst in Mg-O_2 cells.[49]

■ ASSOCIATED CONTENT

Supporting Information

Cyclic voltammetry (CV) of TEMPO in Ar, determination of the diffusion coefficient D_T by chronoamperometry (CA), determination of oxygen solubility; calculations for the oxygen consumption and gas evolution based on the monitoring of the cell pressure, oxygen consumption during the first discharge of Li-O_2 cells with and without TEMPO; Raman and ^{1}H NMR spectrum of discharged cathodes with and without TEMPO; first cycle of Li-O_2 cells with and without TEMPO at different current densities, cycling of Li-O_2 cells with TEMPO, TTF, LiI and without dissolved additives. This information is available free of charge via the Internet at http://pubs.acs.org.

■ AUTHOR INFORMATION

Corresponding Author

juergen.janek@phys.chemie.uni-giessen.de

Notes

The authors declare no competing financial interest.

■ ACKNOWLEDGMENTS

This project was supported by the BASF International Network for Batteries and Electrochemistry. B. J. Bergner was supported by a Kekulé studentship of the Funds of the Chemical Industry (FCI, Frankfurt, Germany). The authors thank Dr. P. Hartmann and Dr. B. Luerßen (University of Giessen) for fruitful discussions, B. Westphal (Technical University of Braunschweig) for providing LFP electrodes and Dr. Limei Chen for performing the Raman measurements.

■ REFERENCES

(1) Abraham, K. M.; Jiang, Z. *J. Electrochem. Soc.* **1996**, *143*, 1.
(2) Girishkumar, G.; McCloskey, B.; Luntz, A. C.; Swanson, S.; Wilcke, W. *J. Phys. Chem. Lett.* **2010**, *1*, 2193.
(3) Xia, C.; Waletzko, M.; Peppler, K.; Janek, J. *J. Phys. Chem. C* **2013**, *117*, 19897.
(4) Lu, Y.-C.; Gallant, B. M.; Kwabi, D. G.; Harding, J. R.; Mitchell, R. R.; Whittingham, M. S.; Shao-Horn, Y. *Energy Environ. Sci.* **2013**, *6*, 750.
(5) Bruce, P. G.; Freunberger, S. A.; Hardwick, L. J.; Tarascon, J.-M. *Nat. Mater.* **2012**, *11*, 19.
(6) Christensen, J.; Albertus, P.; Sanchez-Carrera, R. S.; Lohmann, T.; Kozinsky, B.; Liedtke, R.; Ahmed, J.; Kojic, A. *J. Electrochem. Soc.* **2012**, *159*, R1.
(7) Gallagher, K. G.; Goebel, S.; Greszler, T.; Mathias, M.; Oelerich, W.; Eroglu, D.; Srinivasan, V. *Energy Environ. Sci.* **2014**, *7*, 1555.
(8) Peng, Z.; Freunberger, S. A.; Chen, Y.; Bruce, P. G. *Science* **2012**, *337*, 563.
(9) Laoire, C. O.; Mukerjee, S.; Plichta, E. J.; Hendrickson, M. A.; Abraham, K. M. *J. Electrochem. Soc.* **2011**, *158*, A302.
(10) Black, R.; Oh, S. H.; Lee, J.; Yim, T.; Adams, B.; Nazar, L. F. *J. Am. Chem. Soc.* **2012**, *134*, 2902.
(11) Peng, Z.; Freunberger, S. A.; Hardwick, L. J.; Chen, Y.; Giordani, V.; Bardé, F.; Novák, P.; Graham, D.; Tarascon, J.-M.; Bruce, P. G. *Angew. Chem., Int. Ed.* **2011**, *50*, 6351.
(12) Viswanathan, V.; Thygesen, K. S.; Hummelshøj, J. S.; Nørskov, J. K.; Girishkumar, G.; McCloskey, B. D.; Luntz, A. C. *J. Chem. Phys.* **2011**, *135*, 214704.
(13) Ottakam Thotiyl, M. M.; Freunberger, S. A.; Peng, Z.; Bruce, P. G. *J. Am. Chem. Soc.* **2013**, *135*, 494.
(14) McCloskey, B. D.; Speidel, A.; Scheffler, R.; Miller, D. C.; Viswanathan, V.; Hummelshøj, J. S.; Nørskov, J. K.; Luntz, A. C. *J. Phys. Chem. Lett.* **2012**, *3*, 997.
(15) Xu, J.-J.; Wang, Z.-L.; Xu, D.; Zhang, L.-L.; Zhang, X.-B. *Nat. Commun.* **2013**, *4*, 2438.
(16) Lu, J.; Lei, Y.; Lau, K. C.; Luo, X.; Du, P.; Wen, J.; Assary, R. S.; Das, U.; Miller, D. J.; Elam, J. W.; Albishri, H. M.; El-Hady, D. A.; Sun, Y.-K.; Curtiss, L. A.; Amine, K. *Nat. Commun.* **2013**, *4*, 2383.
(17) Shui, J.-L.; Karan, N. K.; Balasubramanian, M.; Li, S.-Y.; Liu, D.-J. *J. Am. Chem. Soc.* **2012**, *134*, 16654.
(18) Suntivich, J.; May, K. J.; Gasteiger, H. A.; Goodenough, J. B.; Shao-Horn, Y. *Science* **2011**, *334*, 1383.
(19) Xu, J.-J.; Xu, D.; Wang, Z.-L.; Wang, H.-G.; Zhang, L.-L.; Zhang, X.-B. *Angew. Chem., Int. Ed.* **2013**, *52*, 3887.
(20) Lee, J.-H.; Black, R.; Popov, G.; Pomerantseva, E.; Nan, F.; Botton, G. A.; Nazar, L. F. *Energy Environ. Sci.* **2012**, *5*, 9558.
(21) Chase, G. V.; Zecevic, S.; Walker, W.; Uddin, J.; Sasaki, K. A.; Giordani, V.; Bryantsev, V.; Blanco, M.; Addison, D. US Patent Application No. 20120028137 A1 2011.
(22) Hase, Y.; Shiga, T.; Nakano, M.; Takechi, K.; Setoyama, N. US Patent Application No. US 2009/0239113 A1 2009.
(23) Chen, Y.; Freunberger, S. A.; Peng, Z.; Fontaine, O.; Bruce, P. G. *Nat. Chem.* **2013**, *5*, 489.
(24) Lim, H.-D.; Song, H.; Kim, J.; Gwon, H.; Bae, Y.; Park, K.-Y.; Hong, J.; Kim, H.; Kim, T.; Kim, Y. H.; Lepró, X.; Ovalle-Robles, R.; Baughman, R. H.; Kang, K. *Angew. Chem., Int. Ed.* **2014**, *53*, 4007.
(25) Zhao, M.; Li, J.; Mano, E.; Song, Z.; Reider, P. J. *J. Org. Chem.* **1999**, *64*, 2564.
(26) Dijksman, A.; Marino-González, A.; Mairata I Payeras, A.; Arends, I. W.; Sheldon, R. A. *J. Am. Chem. Soc.* **2001**, *123*, 6826.
(27) Sheldon, R. A.; Arends, I. W. C. E. *Adv. Synth. Catal.* **2004**, *346*, 1051.
(28) Georges, M. K.; Veregin, R. P. N.; Kazmaier, P. M.; Hamer, G. *Macromolecules* **1993**, *26*, 2987.
(29) Hawker, C. J. *J. Am. Chem. Soc.* **1994**, *116*, 11185.
(30) Pattison, D. I.; Lam, M.; Shinde, S. S.; Anderson, R. F.; Davies, M. J. *Free Radical Biol. Med.* **2012**, *53*, 1664.
(31) Buhrmester, C.; Moshurchak, L. M.; Wang, R. L.; Dahn, J. R. *J. Electrochem. Soc.* **2006**, *153*, A1800.
(32) Hase, Y.; Ito, E.; Shiga, T.; Mizuno, F.; Nishikoori, H.; Iba, H.; Takechi, K. *Chem. Commun.* **2013**, *49*, 8389.
(33) Bender, C. L.; Hartmann, P.; Vračar, M.; Adelhelm, P.; Janek, J. *Adv. Energy Mater.* **2014**, 1301863.
(34) McCloskey, B. D.; Scheffler, R.; Speidel, A.; Girishkumar, G.; Luntz, A. C. *J. Phys. Chem. C* **2012**, *116*, 23897.
(35) Hodgson, J. L.; Namazian, M.; Bottle, S. E.; Coote, M. L. *J. Phys. Chem. A* **2007**, *111*, 13595.
(36) Chabita, P. C.; Mandal, K. *Indian J. Chem.* **2002**, *41A*, 2231.

(37) Bard, A. J.; Faulkner, L. R. *Electrochemical Methods. Fundamentals and Applications*, 2nd ed.; Harris, D., Ed.; John Wiley & Sons: Hoboken, 2001; pp 156−168.
(38) Hartmann, P.; Grübl, D.; Sommer, H.; Janek, J.; Bessler, W. G.; Adelhelm, P. *J. Phys. Chem. C* **2014**, *118*, 1461.
(39) Kraytsberg, A.; Ein-Eli, Y. *J. Power Sources* **2011**, *196*, 886.
(40) Adams, B. D.; Radtke, C.; Black, R.; Trudeau, M. L.; Zaghib, K.; Nazar, L. F. *Energy Environ. Sci.* **2013**, *6*, 1772.
(41) McCloskey, B. D.; Valery, A.; Luntz, A. C.; Gowda, S. R.; Wallra, G. M.; Garcia, J. M.; Mori, T.; Krupp, L. E. *J. Phys. Chem. Lett.* **2013**, *4*, 2989.
(42) Freunberger, S. A.; Chen, Y.; Drewett, N. E.; Hardwick, L. J.; Bardé, F.; Bruce, P. G. *Angew. Chem., Int. Ed.* **2011**, *50*, 8609.
(43) Freunberger, S. A.; Chen, Y.; Peng, Z.; Griffin, J. M.; Hardwick, L. J.; Bardé, F.; Novák, P.; Bruce, P. G. *J. Am. Chem. Soc.* **2011**, *133*, 8040.
(44) McCloskey, B. D.; Bethune, D. S.; Shelby, R. M.; Girishkumar, G.; Luntz, A. C. *J. Phys. Chem. Lett.* **2011**, *2*, 1161.
(45) Mikhaylik, Y. V.; Akridge, J. R. *J. Electrochem. Soc.* **2004**, *151*, A1969.
(46) Busche, M. R.; Adelhelm, P.; Sommer, H.; Schneider, H.; Leitner, K.; Janek, J. *J. Power Sources* **2014**, *259*, 289.
(47) Hartmann, P.; Bender, C. L.; Vračar, M.; Dürr, A. K.; Garsuch, A.; Janek, J.; Adelhelm, P. *Nat. Mater.* **2013**, *12*, 228.
(48) Sun, D.; Shen, Y.; Zhang, W.; Yu, L.; Yi, Z.; Yin, W.; Wang, D.; Huang, Y.; Wang, J.; Wang, D.; Goodenough, J. B. *J. Am. Chem. Soc.* **2014**, *136*, 8941.
(49) Shiga, T.; Hase, Y.; Yagi, Y.; Takahashi, N.; Takechi, K. *J. Phys. Chem. Lett.* **2014**, *5*, 1648.